Nat Hazards (2011) 58:117–140
DOI 10.1007/s11069-010-9653-z

ORIGINAL PAPER

Risk analysis for flood-control structure under consideration of uncertainties in design flood

Shiang-Jen Wu · Jinn-Chuang Yang · Yeou-Koung Tung

Received: 14 July 2010 / Accepted: 22 October 2010 / Published online: 9 November 2010

Abstract This study presents a risk analysis model to evaluate the failure risk for the flood-control structures in the Keelung River due to the uncertainties in the hydrological and hydraulic analysis, including hydrologic, hydraulic, and geomorphologic uncertainty factors. This study defines failure risk as the overtopping probability of the maximum water level exceeding the levee crown, and the proposed risk analysis model integrates with the advanced first-order and second-moment (*AFOSM*) method to calculate the overtopping probability of levee system. The proposed model is used to evaluate the effects of the freeboard and flood-diversion channel on the flood-control ability of the levees in the Keelung River, which were designed based on the 3-day, 200-year design rainfall event. The numerical experiments indicate that the hydrologic uncertainty factors have more effect on the estimated maximum water level than hydraulic and geomorphologic uncertainty factors. In addition, the freeboard and the flood-diversion channel can effectively reduce the overtopping probability so as to significantly enhance the flood-control capacity of the levee system in the Keelung River. Eventually, the proposed risk analysis successfully quantifies the overtopping risk of the levee system under a scenario, the increase in the average 200-year rainfall amount due to climate change, and the results could be useful when planning to upgrade the existing levee system.

Keywords Design flood · Overtopping probability · Multivariate Monte Carlo simulation · Advanced first-order second-moment (AFOSM) · Climate change

S.-J. Wu (✉)
National Center for High-Performance Computing, Hsinchu, Taiwan
e-mail: sjwu@nchc.org.tw

J.-C. Yang
Department of Civil Engineering, National Chiao Tung University, Hsinchu, Taiwan
e-mail: jcyang@mail.nctu.edu.tw

Y.-K. Tung
Department of Civil and Environmental Engineering, Hong Kong University of Science and Technology, Clear Water Bay, Hong Kong
e-mail: cetung@ust.hk

1 Introduction

The flow carrying capacity of a flood-control structure is determined on the basis of a design flood for a specific return period. In general, the design flood magnitude is estimated by the frequency analysis using observed runoff data. However, in regions without streamflow gauges or with insufficient runoff data, the design flood is generally estimated by adopting a design rainfall event of a specific return period through the hydrological and hydraulic routing. Since a rainstorm event is characterized by the rainfall amount, duration and storm pattern (Wu et al. 2006), the design rainfall event is established by combining the design rainfall amount and storm pattern for a particular duration. The design rainfall amount is calculated using the frequency analysis while the design storm pattern, which defines the temporal distribution of the rainfall, can be produced either from the observed rainfall events or synthetically. Thus, the design rainfall hyetograph can be established by combining the design rainfall amount and the storm pattern for estimating the runoff hydrograph through the use of the rainfall-runoff model. Determination of the design flood requires an estimation of the design rainstorm event of a specific return period and parameters-calibration in the rainfall-runoff model. Using the design flood, the resulting maximum water level from the hydraulic model can be obtained for determining the capacity or dimension of flood-control hydraulic structures, such as the height of the embankment for a levee system.

However, imperfect knowledge about the analysis procedure and data result in uncertainty in the estimation of floods (Smith and Ward 1998). This could lead to failure probability of the practical flood exceeding the design value resulting in potential destruction of the flood-control structure, so that implementation of the risk analysis for the hydraulic structures is essential. Yen (1970) suggested that the return period of the hydrological design can be determined using the probability theory if the project life and simple risk, due to the limited record of rainfall data, are known. Tung (1985) explored the flow conveyance reliability of hydraulic structures using two generalized dynamic reliability models with hydrological and hydraulic uncertainties. Lee and Mays (1986) analyzed the failure probability of flood levee capacity due to the hydraulic uncertainty of Manning's equation using a first-order analysis. Anselmo et al. (1996) proposed a risk assessment framework for a flood-prone area to analyze the effects of the flood events. The proposed framework integrated the hydrological and hydraulic modeling, and its detailed framework simulated the flooded area using the two-dimensional hydraulic model with the boundary conditions calculated by the rainfall-runoff model and considering the extreme and PMP value of the rainfall. Salas et al. (2003) proposed a risk assessment procedure to quantify the failure probability of hydraulic structures due to hydrological uncertainties using the method of moments (MOM), probability-weighted moments (PWM), and maximum likelihood (ML) under an assumption that the underlying probability distribution is the Gumbel. Hadiani and Ebadi (2007) performed a risk assessment for the hydraulic structures resulting from the uncertainty in the design flood due to change in land-use and capacity, defined as the environmental factors. Apel et al. (2004, 2006) proposed a simple but efficient dynamic probabilistic method to evaluate dike failure probability. The proposed method quantified the cumulated flood risk by simulating the complete chain of flooding process by a Monte Carlo framework based on actual flooding events, rather than hypothetical scenarios. Also, the proposed dynamic probabilistic model was applied to explore the influence of dike breaches on flood frequency distribution along rivers (Apel et al. 2009).

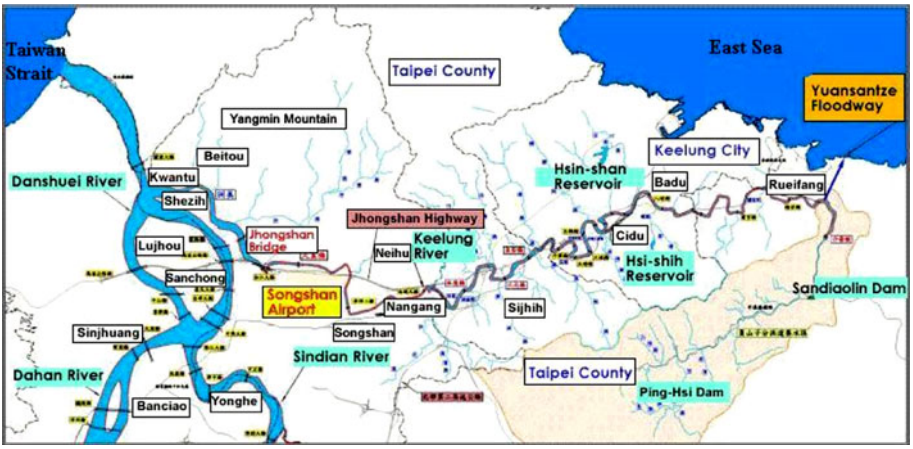

Fig. 1 Keelung River watershed and neighboring basins (WRA, 2005)

The above-mentioned literature primarily focuses on the effect of single (hydrological, hydraulic, or geomorphic factors) or composited uncertainties (hydrological and hydraulic factors) for the risk analysis of hydraulic structures. The risk analysis model proposed herein primarily takes into account hydrologic, hydraulic, and geomorphic uncertainties to explore the reliability of the flood-control structures in the fluvial system. Since levees are widely used to protect urban and watershed areas from being flooded, this study focuses on a risk analysis for the flood-control ability of a dike system in order to calculate the failure probability of the water level exceeding the embankment. The Keelung River, located in Northern Taiwan, is chosen as the study area (see Fig. 1). The reliability of the dike system is evaluated under the design flood with the peak discharge of a 200-year return period. This study not only analyzes the sensitivity of the hydrologic, hydraulic, and geomorphic uncertainty factors as related to the flood-control capacity of levees along the Keelung River, but it also evaluates the performance of the freeboards and the flood-diversion channel and their impact on the flood-control ability of the levee system using the proposed risk analysis model.

2 Risk analysis model

In the past, the definition of the risk is a failure probability, such as the probability of water level rising over the levee, and it is named as the classical risk. Since floods frequently result in direct and indirect damage of human life and properties. Recently, the term "risk" is used to take into account the consequence, such as the inundation area or damage, and it is expressed as the product of the probability and consequence (Gouldby et al. 2005). Mays (2001) presented a five-step risk assessment: (1) risk or hazard identification; (2) assessment of loads and resistance; (3) uncertainty analysis; (4) quantification of the composite risk; and (5) development of composite risk-safety factor relationship. The type of risk must be identified in advance. This study adopts the classical risk, i.e. the failure probability. Tung and Mays (1981) indicated that the risk for hydrologic and hydraulic analysis can be expressed as follows:

$$\text{Risk} = \Pr[R > L] \tag{1}$$

where Pr(•) refers to overtopping probability that loading (L) is greater than the resistance (R). For the flood-control ability of the levee, R and L can be, respectively, the maximum water level and the crown elevation of the levee, and Eq. 1 can be rewritten as,

$$\text{Risk} = \Pr[H_{\max} > h^*] \tag{2}$$

where $H_{\max}$ denotes the maximum water level, and h^* represent the height of the embankment crown.

Several uncertainty and risk methods are used in the reliability assessment of the water resource engineering systems, such as the mean first-order second-moment (*MFOSM*), the advance first-order second-moment (*AFOSM*) and the Monte Carlo simulation (*MCS*) method. Since *AFOSM* method primarily focuses on the risk assessment under a failure situation, it is more appropriate for the safety assessment of hydraulic structures. Thus, this study employs *AFOSM* to calculate the probability of maximum water level overtopping the embankment due to the uncertainties which dominate the estimation of the maximum water level in the hydrological and hydraulic analysis. For *AFOSM* method, a relationship must be established between the uncertainty factors and the corresponding model outputs; thus, this study applies the Monte Carlo simulation method to generate the uncertainty factors and then imports them into the models to obtain the model outputs. The relationship between the maximum water level and the uncertainty factors could be established using the multivariate regression analysis.

2.1 Framework of the proposed risk analysis model

Referring to the Tung and Mays (1981) risk assessment procedure, the proposed framework of the risk analysis model in this study can be briefly summarized as follows:

Step [1]: Identify the uncertainty factors resulting in the risk of the water level rising over the levees crown along the river.
Step [2]: Generate the uncertainty factors using the Monte Carlo simulation.
Step [3]: Estimate the maximum water level through the rainfall-runoff modeling and hydraulic routing.
Step [4]: Establish the relationship between the water level and the uncertainty factors using the multivariate regression analysis.
Step [5]: Calculate the overtopping probability over the levee crown using *AFOSM*.

Each of steps in the risk model is detailed below.

2.2 Identify uncertainty factors

Flood disaster mitigation strategies are based on a comprehensive assessment of the flood risk combined with a thorough study of the uncertainties associated with the risk assessment procedure (Apel et al. 2004). Based on the above procedure of risk analysis proposed by Tung and Mays (1981), the uncertainty factors can be grouped into three types: (1) inherent uncertainty due to the random nature of the processed involved (e.g. Yen 1970); (2) model uncertainty resulting from the lack of complete information on the process; and (3) parameter uncertainty due to an insufficient amount of data from which the parameters in an assumed model are estimated, such as the parameters of the rainfall-runoff model (e.g. Uhlenbrook et al. 1999; Yu et al. 2001) and the Manning's roughness coefficient of a

hydraulic routing (e.g. Lee and Mays 1986). Except for model uncertainty, this study treats the uncertainties in the data, model parameters and land-use of a watershed as the uncertainty factors affecting the design flood.

Since the water level results from the hydrologic and hydraulic routing with the design rainfall of a specific return period, its reliability is affected by the uncertainties in the process of these routings and inputs. In general, the uncertainty factors in the hydrologic and hydraulic routings involve the design rainfall amount, storm pattern, infiltration, parameters of rainfall-runoff and hydraulic models, such as Manning's roughness coefficient, the coefficients of the flow regulating structures, (e.g. the weir coefficient), and the boundary conditions (e.g. the downstream tide level and upstream runoff hydrograph). The upstream boundary runoff hydrograph is commonly estimated through a rainfall-runoff model, so that its uncertainty should be resulted from the uncertainty in model parameters and design rainstorm. In addition, since the environmental factors, such as the land-use of a watershed, affect the design flood (Hadiani and Ebadi 2007), it is necessary to evaluate the effect of the change in land-use such as urbanization, which influences the infiltration capacity on the design flood. Hence, this study employs the curve number (*CN*) method to calculate the infiltration based on the curve number of a catchment corresponding to the land-use and vegetation coverage with the *CN* value being uncertain. In summary, this study takes into account eight uncertainty factors, including a 200-year rainfall amount, storm pattern, parameters of the rainfall-runoff model, downstream tide level, coefficients of hydraulic structures (weir coefficient and contraction coefficient of the bridge), Manning's roughness coefficient, and curve number (*CN*).

The primary determinants of flood risks involve factors from hydrology, hydraulics, structural and geotechnical aspects, material and construction, seismology factors, and operation and maintenance (National Research Council 2000). Of the above-mentioned uncertainties, the hydrological factors include rainfall, runoff, and basin as well as channel data. The hydraulic factors are the characteristics of floodwater propagation and the equations and methods used to simulate such propagation. The structural and geotechnical factors refer to the geographical and geological characteristics of the ground and soils. Therefore, based on the characteristics and impact of uncertainties, this study classifies the eight uncertainty factors considered into three types, i.e. the hydrological, hydraulic, and geomorphologic factors as listed in Table 1.

Table 1 Classification of uncertainty factors considered

Type	Impact	Factor
Hydrological factors	Design rainfall amount and total runoff	Design rainfall amount
		Storm pattern
		Parameters of rainfall-runoff model
Hydraulic factors	River stage	Tide level
		Weir coefficient
		Contraction coefficient of the bridge
		Roughness coefficient
Geographical factors	Infiltration	Land-use and vegetation coverage

2.3 Generation of uncertainty factors

Theoretically, the hydrological, hydraulic, and geomorphologic factors have different physical and statistical characteristics. As a result, this study generates the uncertainty factors using the Monte Carlo simulation based on their physical and statistical properties. Specifically, since the *CN* belongs to the integer value, it is produced by the bootstrap re-sampling method with a reasonable range in this study. The generation of the uncertainty factors is described below.

2.3.1 Hydrological uncertainty factors

The hydrological uncertainty factors include the design rainfall amount of a specific return period, the storm pattern, and the parameters of the rainfall-runoff model. The design rainfall amount and storm pattern are combined to define the design rainstorm hyetograph. The duration of a design rainstorm event is commonly determined in advance. For example, the duration of design rainstorm event for the Keelung River basin is 3 days (WRA 2005). The rainfall amount of T-year event is estimated using the frequency analysis, and the design storm pattern is produced based on the statistical properties of observed rainfall hyetographs of major rainstorm events. Their simulations are expressed as follows.

2.3.1.1 Design rainfall amount of a specific period T-year In general, the frequency analysis requires adopting a probability distribution function (*PDF*), which is determined using the statistical test, such as the K–S test. Since this study primarily evaluates the effect of T-year rainfall amount on the capacity or dimension of flood-control hydraulic structures due to uncertainty in the observation, this study adopts a *PDF* consistent with that used in the flood treatments planning. Hence, the probability distribution adopted in the study area, Keelung River, is the Log-Pearson III distribution (WRA 2005). In addition, to quantify the statistical features of the T-year rainfall amount, this study employs the bootstrap re-sampling method along with the frequency analysis on the ransom samples of t-hour annual maximum rainfalls. Using the calculated statistical properties of t-hour maximum rainfalls, the T-year rainfall amount can be generated by means of the Monte Carlo simulation method.

2.3.1.2 Design storm pattern The design storm pattern defines the variation of rainfall over time for a specific duration, such as the 3-day design storm pattern for the study area, Keelung River watershed, as shown in Fig. 2. As shown in Fig. 2, the design storm pattern is a central distribution of the rainfall in time, and in Taiwan it is commonly estimated using the Chicago model (Keifer and Chu 1957) or the Gauss–Markov methods (Cheng et al. 2001). Wu et al. (2006) presented that the storm pattern is composed of the dimensionless rainfalls, in which two special features must be observed: (1) the sum of the dimensionless rainfalls must be equal to one. $P_{0.1} + P_{0.2} + \cdots + P_{1.0} = 1$ as $0 \le F_{0.1} \le F_{0.2} \le \cdots \le F_{1.0} = 1$ and (2) dimensionless rainfalls must be between zero and one $0 \le P_t \le 1$ (Wu et al. 2006). This study adopts the above-mentioned dimensionless rainfall hyetograph as the design storm pattern. According to the above two special features, the ordinates of the dimensionless rainfall P_t must be considered as the correlated non-normal random variables. Therefore, this study adopts the multivariate Monte Carlo simulation with the Johnson distribution (Wu et al. 2006) to generate the dimensionless rainfalls of the central design storm pattern.

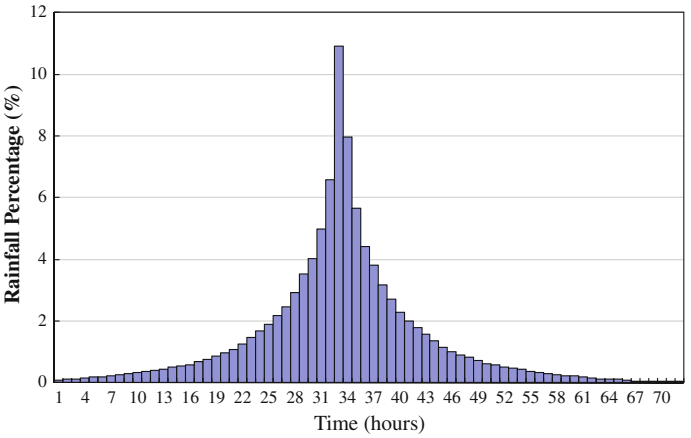

Fig. 2 Dimensionless 3-day design storm pattern for Keelung River watershed

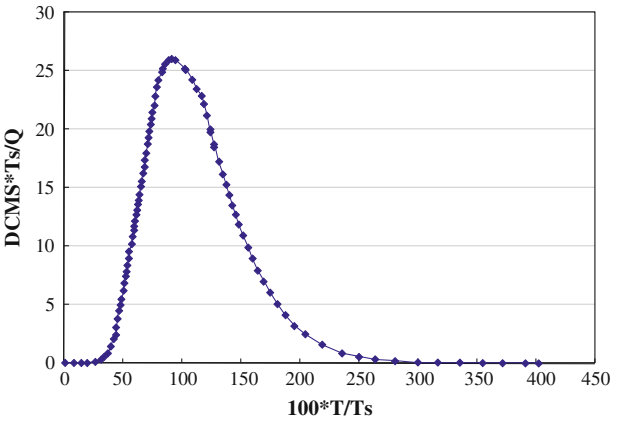

Fig. 3 Dimensionless unit hydrograph for Keelung River watershed

2.3.1.3 Parameters of runoff-runoff model To estimate the design flood, a rainfall-runoff model is needed to produce the hydrograph corresponding to the design rainfall hyetograph. The unit hydrograph is widely used for the hydrological analysis (e.g., Schulz et al. 1971; Rodriguez-Iturbe et al. 1982; Yen and Lee 1997; Chou and Wang 2002). A number of dimensionless unit hydrographs are widely used for deriving the unit hydrograph at ungauged basins, such as the synthetic unit hydrograph (Snyder 1938), SCS method (Soil Conservation Service 1972), and the geomorphic instantaneous unit hydrograph (Rodriguez-Iturbe et al. 1982; Yen and Lee 1997). Figure 3 shows the dimensionless unit hydrograph commonly adopted in Taiwan (Wu 1965), the horizontal and vertical ordinates of which are defined as follows:

$$\begin{aligned} t^* &= t/T_s; \quad q^* = \mathrm{DCMS} \times T_s/q \\ T_s &= T_{\mathrm{lag}} + \Delta t/2 \end{aligned} \tag{3}$$

in which t^* and q^* are dimensionless time and discharge; t and q are time and discharge (m^3/s); *DCMS* represents the daily runoff volume; and Δt is the time increment of the unit hydrograph. The lag time T_{lag} can be calculated by:

$$T_{\text{lag}} = \alpha_{T_{\text{lag}}} \times \left(\frac{L \times L_{ca}}{\sqrt{s}}\right)^{\beta_{T_{\text{lag}}}} \tag{4}$$

where $\alpha_{T_{\text{lag}}}$ and $\beta_{T_{\text{lag}}}$ are coefficients for the basins related with the geomorphologic features of the watershed; and L and L_{ca} are the length of a river and the distance from outlet of the river to the gravity of the catchment, respectively. In the case of α and β being known, the horizontal and vertical coordinates of a unit hydrograph can be transformed through Eq. 3. Since the lag time equation Eq. 3 is derived from the regression analysis, the estimations from the regression equation probably differ from the observed data. Hence, the regression equation generally cannot go through all the data, so that the results from the regression equation entail error. Therefore, this study takes into account the uncertainty of the regression equation. Thus, Eq. 3 is rewritten as

$$\begin{aligned} T_{\text{lag}} &= \alpha^*_{T_{\text{lag}}} \times \left(\frac{L \times L_{\text{ca}}}{\sqrt{s}}\right)^{\beta_{T_{\text{lag}}}} \\ \alpha^*_{T_{\text{lag}}} &= e^{\ln\left(\alpha_{T_{\text{lag}}}\right)+\varepsilon_{T_{\text{lag}}}} \end{aligned} \tag{5}$$

where $\varepsilon_{T_{\text{lag}}}$ is the regression error. In this study, the modified coefficient $\alpha^*_{T_{\text{lag}}}$ is defined as the uncertainty factors and simulated by the Monte Carlo simulation method with mean and standard deviation of 0 and 1, respectively. In the Keelung River study area, the coefficients of the lag time account for $\alpha_{T_{\text{lag}}} = 0.15$ and $\beta_{T_{\text{lag}}} = 0.37$.

2.3.2 *Generation of hydraulic uncertainty factors*

In Table 1, the hydraulic uncertainty factors are the downstream boundary condition (tide level), coefficients of hydraulic structures (weir coefficient and contraction coefficient of the bridge), and Manning's roughness coefficient. The above-mentioned uncertainty factors are related to the river stage. Their generation is described below.

2.3.2.1 Downstream boundary (tide level) Hydraulic routing requires two boundary conditions, i.e. lateral/upstream and downstream conditions. The upstream and lateral boundary conditions are generally given in terms of the runoff hydrograph, whereas the downstream boundary is specified by the water level, such as the tide level. In this study, the runoff hydrograph can be obtained using the rainfall-runoff routing with the generated uncertainty factors, whereas the tide levels are simulated by the Monte Carlo method with the statistics of the tide depth resulting from the typhoon events.

2.3.2.2 Weir coefficient The weir formula describes the lateral discharge through the weir and is expressed as:

$$Q_{\text{weir}} = \alpha_{\text{weir}} \times L \times (H - H_0)^{\beta_{\text{weir}}} \tag{6}$$

where α_{weir} and β_{weir} are the coefficients; and L and H_0 denote the length and crest elevation of the weir. When the water level is greater than H_0, the weir starts providing the discharge. The same as the lag time equation, Eq. 3, this study considers the uncertainty in the form of the regression equation, so that Eq. 5 can be rewritten as

$$Q_{\text{weir}} = \alpha^*_{\text{weir}} \times (H - H_0)^{\beta_{\text{weir}}}$$
$$a^*_{\text{weir}} = e^{\ln(L \times a_{\text{weir}}) + \varepsilon_{\text{weir}}} \tag{7}$$

where $\varepsilon_{\text{weir}}$ denotes the error in weir flow equation, the mean and standard deviation of which are 0 and 1; and a^*_{weir} is the modified coefficient. In this study, a^*_{weir} is defined as the uncertainty factors and generated by the Monte Carlo simulation method. For the Keelung River study area, the coefficients of the weir equation are $\alpha_{\text{weir}} = 1.41$ and $\beta_{\text{weir}} = 1.96$.

2.3.2.3 Manning's roughness coefficient and contraction coefficient of bridge Similarly, this study generates the contraction coefficient of the bridge (c_c) and the Manning's roughness coefficients for the main channel (N_c) and flooding plain (N_f) using the Monte Carlo simulation method. Nevertheless, it is difficult to obtain their statistical moments. Therefore, as for the contraction coefficients of the bridges (c_c), this study adopts its mean and standard deviation by referring to the design report. Moreover, this study adopts the various statistics of Manning's roughness coefficients at the main channel and flooding area according to the flooding treatment report of the watershed. Thus, c_c, n_c, and n_f are also reproduced using the Monte Carlo simulation.

2.3.3 Geomorphologic uncertainty factor

The geomorphologic uncertainty factors considered herein is the curve number (*CN*) that relates to the land-use and vegetation coverage. Using the curve number model, the infiltration can be estimated by (Soil Conservation Service 1972):

$$P_e = \frac{(P - 0.2S)^2}{(P + 0.8S)}$$
$$S = \left(\frac{1000}{\text{CN}} - 10\right) \times 25.4 \tag{8}$$

where P and P_e denote the total and effective rainfall amount; and S is the parameter. Changes in land-use and vegetation coverage of the watershed, such as urbanization, alter the *CN* value and the corresponding value of the design flood. Hence, this study reproduces the *CN* value by means of the bootstrap re-sampling method with a reasonable range determined based on the land-use change in a watershed.

In summary, the generated T-year rainfall amount and the design storm pattern are combined to define the generated design hyetograph. By integrating it with the corresponding Eq. 8 with the generated *CN*, the design effective hyetograph can be obtained. As the generated effective hyetograph is input into rainfall-runoff model with the simulated parameters, the corresponding simulated runoff hydrograph could be produced. Using the estimated runoff hydrograph and tide level, the water-level hydrographs at various cross-sections of interest along the river can be calculated through the hydraulic routing. Many numerical models can be applied for the hydraulic routing, such as HEC-RSA and SOBEK, or MIKE 11. SOBEK is a sophisticated one-dimensional open-channel dynamic flow modeling system (WL|Delft Hydraulic 2005). It can be used to simulate and tackle problems in river management, flood protection, design of canals, irrigation systems, water quality, navigation, and dredging. This study adopts SOBEK model for the hydraulic simulation of the water level in the river network.

2.4 Establishing the maximum level relationship

This study evaluates the risk of the maximum water level exceeding the levee crown using the advanced first-order and second-moment (*AFOSM*) method. The *AFOSM* requires a functional relationship between the maximum water level and the corresponding hydrological, hydraulic, and geomorphic uncertainty factors, which must be established using the multivariate regression analysis. Of uncertainty factors considered, the storm pattern is composed of dimensionless rainfalls. Hence, it is necessary to select a suitable dimensionless rainfall to represent the entire storm pattern in establishing maximum water-level relationship. For maximum water level, it is reasonable to judge that the maximum rainfall intensity in terms of the rainfall amount and maximum dimensionless rainfall would be a significant factor. Therefore, this study adopts the maximum dimensionless rainfall as the variable representing the storm pattern to derive the maximum water-level relationship by the multivariate regression method as:

$$H_{\max} = f_h\left(\theta_{\text{hydro}}, \theta_{\text{hydra}}, \theta_{\text{geo}}\right) \tag{9}$$

where $f_h(\bullet)$ is a general function relation; $H_{\max}$ denotes the maximum water level; and θ_{hydro}, θ_{hydra}, and θ_{geo} are the hydrological, hydraulic, geomorphologic uncertainty factors, respectively.

2.5 Calculation of overtopping probability

The *AFOSM* is employed to analyze the failure risk of the flood-control structures attributed to the hydrological, hydraulic, and geographical uncertainty factors. In this study, the failure risk is defined as the overtopping probability of the maximum water level rising over the embankment crown (see Eq. 2), which can be expressed as:

$$\text{Risk} = P_r(H_{\max} > h^*) = P_r[Z > 0] = \Phi(-\beta) \tag{10}$$

in which $Z = H_{\max} - h^*$ and h^* denote the performance function and the levee crown; $\Phi(\bullet)$ represents the standard normal distribution; and $\beta = \frac{E(z)}{s_z}$ is the reliability index with $E(z)$ and s_z being the mean and standard deviation of Z. The mean and standard deviation of performance for Z can be estimated by:

$$\begin{aligned} E(z) &= H_{\max,x^*} + \sum_{i=1}^{m} \left|\frac{\partial H_{\max}}{\alpha X_i}\right|_{x_i^*} (\mu_{x_i} - x_i^*) - h^* \\ s_z &= \sqrt{\sum_{i=1}^{m} \left(\frac{\partial H_{\max}}{\partial X_i}\right)^2 \sigma_{x_i*}^2} \end{aligned} \tag{11}$$

where x_i^* denotes the failure points of the ith uncertainty factor when the performance function $Z = 0$; μ_{x_i} and σ_{x_i} are the mean and standard deviation of the ith uncertainty factor; and $H_{\max,x^*}$ denotes the maximum peak water level evaluated at the failure points of uncertainty factors x^*. Note that $\frac{\partial H_{\max}}{\partial X_i}$ is the sensitivity coefficient. Using Eq. 11, the overtopping probability $\Phi(-\beta)$ can be calculated with the given mean and variance of the uncertainty factors.

2.6 Study area

Referring to Fig. 1, the Keelung River starts from Jingtong Mountain, Ping-Shi township, Taipei County, and joins the Danshuei River in the Kwantu area of Taipei City. The river is

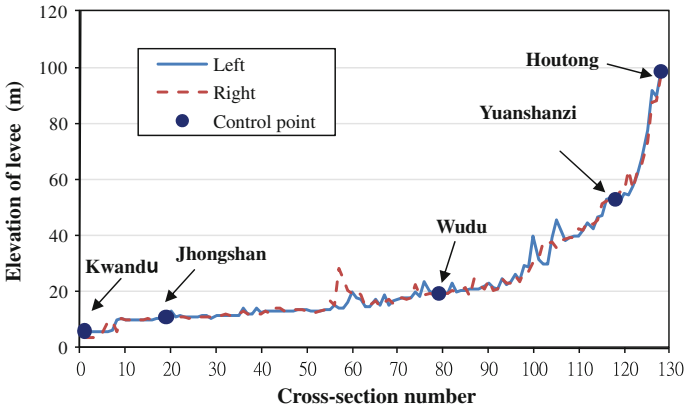

Fig. 4 Elevation of levees on left and right banks and locations of control points in Keelung River

86.4 km long, with a basin area totaling 491 km^2. The Keelung River is one of the three main branches of the Danshuei River; and the other two branches are the Dahan River and the Sindein River. The design flood for the flood-control hydraulic structures in the Keelung River has a 200-year return period. To effectively achieve flood control, the Keelung River Overall Improvement Early Stage Project was proposed with a budget of 31.6 billion NT dollars. This project includes Yuanshanzi flood diversion, construction of dikes, water gates and pumping stations, reconstruction of bank protection bridges, water and soil conservation, flood forecast and inundation alarm system establishment. The Yuanshanzi Diversion Project plays an important role in the whole project by diverting 1,310 m^3/sec in peak from the upper Keelung River into the East Sea. Along with the other flood-control measures, such as dikes, pumping stations, and watershed conservation works, the diversion project made it possible for the Keelung River to achieve the criteria of the 200-year flood protection. Figure 4 shows the elevation of the levees on the left and right banks and the locations of the control points in the Keelung River.

3 Result and discussion

3.1 Basic conditions of risk analysis

According to the Flood Protection and Mitigation Plan of the Keelung River (WRA 2005), the design flood is the one whose the maximum water level resulting from a 3-day, 200-year rainfall event. To consider the spatial variation of rainfall-runoff characteristics, four control points in which the peak discharge are used for the design of flood-control structures are set up along the Keelung River: Kwantu, Jhongshan Bridge, Wudu, and Yunshanzi.

The 200-year rainfall amounts for the 3-day duration at the four control points were calculated by the frequency analysis on the annual maximum 3-day rainfalls recorded in 1912 to 2007 and then convolve with the unit hydrograph method to obtain the runoff hydrographs at twenty-one tributaries. The base-flow is assumed to be 10 m^3/s. The maximum water level at the cross-section along the Keelung River is estimated using the SOBEK one-dimensional hydraulic model. Figure 5 shows the user interface of the

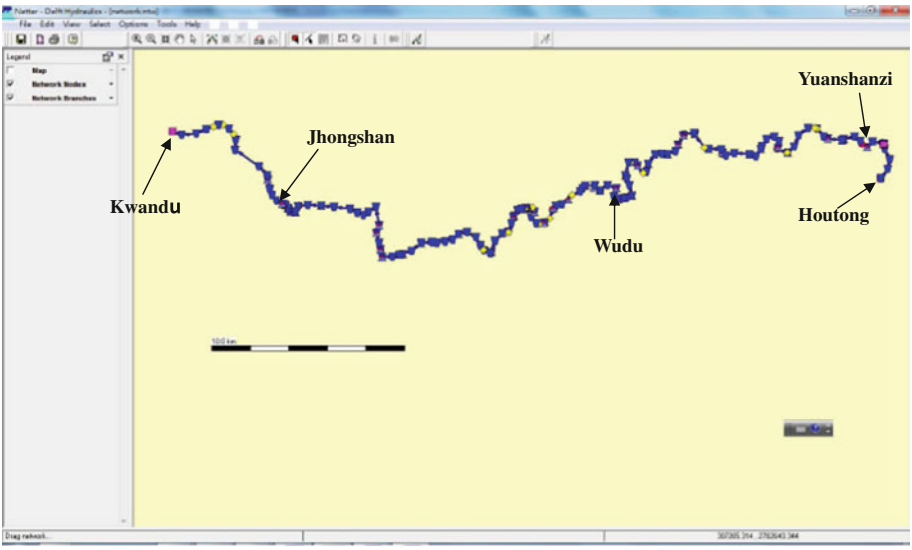

Fig. 5 User interface of Keelung River SOBEK model

SBOEK model for the Keelung River, the downstream and upstream boundaries of which are Kwandu and Houtong. In the SOBEK model, the runoff hydrographs resulting from the twenty-one tributaries are the upstream and lateral boundary conditions.

As this study adopts topographic data of 128 cross-sections as measured in 2007, any change in the bed form is not taken into account in the risk analysis. Note that four control points Kwantu, Jhongshan Bridge, Wudu, and Yunshanzi are located at the 1st, 19th, 79th, and 125th cross-section. In addition, several flood-control structures, such as the water gates and pumping stations are also ignored in this study.

3.2 Statistical analysis for uncertainty factors

In the proposed risk analysis model, the statistics for the uncertainty factors are given for the generation of the uncertainty factors in advance. Except for the *CN* that is reproduced by the bootstrap re-sampling method with a range of 85 to 95, the other uncertainty factors are generated using the Monte Carlo simulation. In detail, the mean and standard deviation of the 200-year rainfall amount are calculated from 200 repetitions of the frequency analysis with the observed 3-day annual maximum rainfalls through the bootstrap re-sampling method. The statistics of tide level are also calculated using measurement data from typhoon events. The statistics of the remaining parameters are hypothesized based on the literatures or the Flood Regulation Planning Report (WRA 2005). Table 2 lists the means and standard deviations of the uncertainty factors used in the proposed risk analysis model, and Fig. 6 shows the mean and standard deviation of the dimensionless design storm pattern for the Keelung River watershed.

In reality, there exists correlation between the uncertainty factors, such as the 200-year rainfall amounts at the four control points and ordinates of the dimensionless storm hyetograph. Table 3 shows the correlation coefficients of the 3-day, 200-year rainfall amounts at the four control points. The correlation coefficients averagely approach 0.85. Even for Kanwdu and Yanshanzi, the control points associated with the longest distance, their

Table 2 Statistics of uncertainty factors considered

Uncertainty	Mean	SD	Probability distribution
3-day, 200-year effective rainfall amount			
D_KD	861 mm	134.3 mm	Log-Pearson III
D_JS	795 mm	126.4 mm	Log-Pearson III
D_WD	868 mm	118.9 mm	Log-Pearson III
D_YS	928 mm	127.1 mm	Log-Pearson III
TD	4.750	0.440	Log-Normal
Cc	1.053	0.583	Log-Normal
a^*_{weir}	0.003	0.152	Normal
n_c	0.03 ~ 0.06	0.001 ~ 0.0065	Log-Normal
n_f	0.048 ~ 0.089	0.003 ~ 0.02	Shifted Exponential
CN	58 ~ 85		Bootstrap re-sampling method

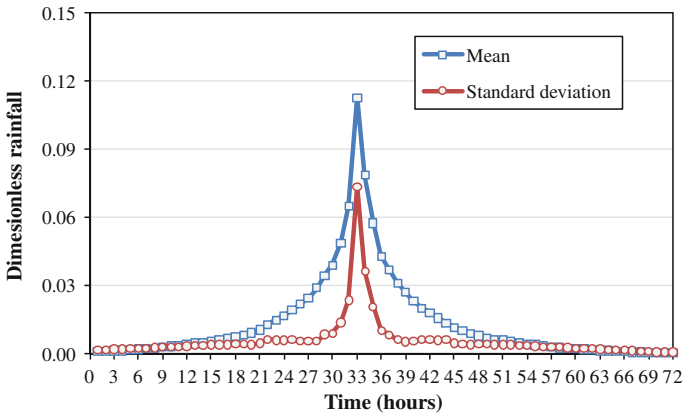

Fig. 6 Mean and standard deviation of dimensionless 3-day design storm pattern for Keelung River watershed

correlation is 0.798. As a result, the 200-year rainfall amounts at the four control points should be treated as spatially correlated variables. Similarly, Table 4 shows the correlation coefficients for t = 1,6,…,72 h and shows that the correlation coefficients vary with time and are between 0.958 and −0.744. This suggests that the dimensionless of dimensionless design hyetograph ordinates rainfall should be temporally correlated variates. Therefore, this study adopts the non-normal correlated multivariate Monte Carlo simulation (Wu et al. 2006), which takes into account the correlation coefficient of the non-normal variables, to simulate the 200-year rainfall amount and dimensionless design storm pattern.

3.3 Relationship of maximum water level with uncertainty factors

The advanced first-order and second-moment (*AFOSM*) method requires a relationship between the maximum water level and uncertainty factors. The T-year rainfall amount and *CN* relate to the estimation of the effective rainfall amount. To simplify the relationship of

Table 3 Correlation coefficients of 3-day, 200-year and rainfall amounts at four control points

Control point	Kwandu	Jhongshan	Wudu	Yuanshanzi
Kwandu	1.000			
Jhongshan	0.970	1.000		
Wudu	0.872	0.909	1.000	
Yuanshanzi	0.798	0.844	0.960	1.000

the maximum water level, this study adopts the 200-year effective rainfall amount. Using 200 generated uncertainty factors from the multivariate Monte Carlo simulation method or the bootstrap re-sampling method, the relationship of the maximum water level can be established by the multivariate regression analysis:

$$H_{\max} = \alpha(D\_KD)^{\beta_1}(D\_JS)^{\beta_2}(D\_WD)^{\beta_3}(D\_YS)^{\beta_4}(NR_P)^{\beta_5}(TD)^{\beta_6}(C_c)^{\beta_7}\left(a^*_{T_{\text{lag}}}\right)^{\beta_8} \times \left(a^*_{\text{weir}}\right)^{\beta_9}(n_c)^{\beta_{10}}\left(n_f\right)^{\beta_{11}} \quad (12)$$

in which the α and β_i (i = 1,11) are the regression coefficients; *D_KD, D_JS, D_WD*, and *D_YS* denote the 200-year effective rainfall amounts at the four control points; NR_P denotes the maximum dimensionless rainfall; *TD*, *Cc*, and a^*_{weir} denote the tide level, contraction coefficient of the bridge and modified weir coefficient, respectively; and *Nc* and N_f are the Manning's roughness coefficients for the main channel and flooding plain. Figure 7 shows the coefficient of determination R^2 of the regression equations at 128 cross-sections. It can be seen that, on average, R^2 exceeds 0.8. As a result, the resulting regression models reasonably represent the relationship between the maximum water level and the uncertainty factors.

Table 5 shows the regression coefficients in the maximum water relationship at four control points, and it can be seen that the regression coefficients β_i of uncertainty factors vary with control points. Since the regression coefficients in Eq. 12 reflect the sensitivity of the uncertainty factors on the maximum water level according to Eq. 11, this study infers the sensitivity of the uncertainty factor to the maximum water level. It is observed that, except for the coefficients of *D_YS* and a^*_{weir}, the coefficients of the remaining uncertainty factors are positive at the Jhongshan, Wudu, and Yuanshanzi. This implies that the maximum water level is negatively related to the 200-year effective rainfall amount at Yuanshanzi and the outflow through the weir. That is, the diversion at Yuanshanzi reduces the discharge in the Keelung River and, hence, lowers the maximum water level accordingly. Additionally, the coefficients of C_c, a^*_{weir}, and N_f are significantly less than those of the other uncertainty factors, implying that their variations have less effect on the estimation of water level than the other uncertainty factors. However, at the Kwandu control point, the regression coefficient associated with the tide level (0.923) significantly dominates those of the remaining uncertainty factors. This is expected as Kwantu is located close to the outlet of Keelung River so that the water level is significantly affected by the tide level. In summary, the maximum water level appears to be more sensitive to the hydrologic uncertainty than the hydraulic and geomorphologic uncertainty factors.

3.4 Calculation of overtopping probability

Although the uncertainty factors contribute to failures of the flood-control structures, this study primarily analyzes the overtopping probability of the maximum water level

Table 4 Correlation coefficients of ordinates of dimensionless storm pattern

	t = 1 h	t = 6 h	t = 12 h	t = 18 h	t = 24 h	t = 30 h	t = 36 h	t = 42 h	t = 48 h	t = 54 h	t = 60 h	t = 66 h	t = 72 h
t = 1 h	1												
t = 6 h	0.958	1											
t = 12 h	0.818	0.896	1										
t = 18 h	0.629	0.705	0.9	1									
t = 24 h	0.195	0.199	0.323	0.563	1								
t = 30 h	−0.651	−0.696	−0.734	−0.619	−0.195	1							
t = 36 h	−0.645	−0.691	−0.744	−0.678	−0.350	0.963	1						
t = 42 h	0.104	0.103	0.209	0.454	0.976	−0.134	−0.296	1					
t = 48 h	0.614	0.686	0.877	0.993	0.611	−0.605	−0.672	0.499	1				
t = 54 h	0.781	0.864	0.993	0.92	0.353	−0.727	−0.742	0.238	0.897	1			
t = 60 h	0.944	0.997	0.905	0.713	0.193	−0.701	−0.696	0.095	0.692	0.873	1		
t = 66 h	0.99	0.927	0.776	0.598	0.191	−0.636	−0.629	0.106	0.583	0.739	0.907	1	
t = 72 h	0.832	0.724	0.544	0.379	0.073	−0.459	−0.436	0.022	0.362	0.517	0.706	0.850	1

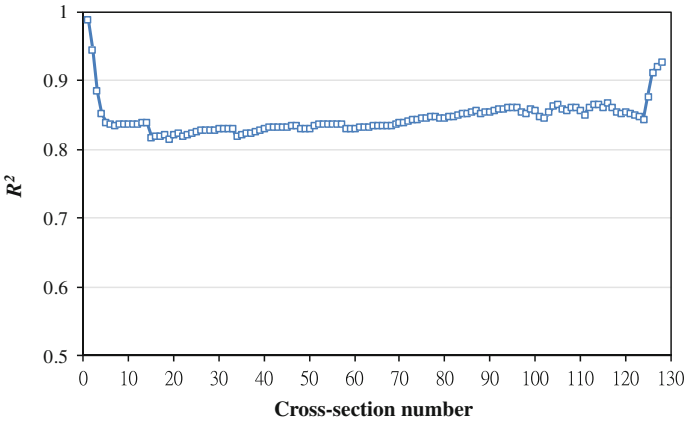

Fig. 7 Coefficient of determination R^2 of relationship of maximum water level at various cross-sections for left and right banks in Keelung River

exceeding the embankment height. Because of the different heights of the river levees, this study calculates the overtopping probability on the left and right banks of the Keelung River.

Generally speaking, in determining the level height based on the design flood, an additional increment of the levee height, named as the freeboard, is required to provide the added protection to the levees during an occurrence of the design flood. In addition, the Yunshanzi flood-diversion channel plays an important role in the flood mitigation plan of the Keelung River. Therefore, this study evaluates the effect of Yuanshanzi diversion channel and the freeboard on the performance of flood-control ability. Finally, this study also analyzes a scenario that assumes that the 200-year rainfall amount increases due to climate change, to demonstrate the applicability of the proposed risk analysis model.

3.4.1 Yuanshinzi flood-diversion channel

According to many references in Taiwan, floodings in the Keelung River mostly are caused by rainstorms at the upstream basins, Huoshaoliao subbasin. Therefore, the Yunshanzi flood-diversion channel was built to divert the runoff (maximum discharge = 1,310 cms) to the East Sea so as to reduce runoff toward the downstream of the Keelung River. To evaluate the effect of the Yuanshanzi diversion channel on the flood control, the overtopping probabilities with and without the diversion are calculated.

Figure 8 shows the overtopping probabilities on the left and right banks of the levees with and without the flood-diversion. It can be observed that the overtopping probabilities with the diversion (on average 0.465) are obviously less than those without it (on average 0.666), especially for the upstream of diversion. Referring to Fig. 4, Table 6 lists the average overtopping probability of four river reaches and entire cross-sections with and without the flow-diversion channel. The four reaches reveal different overtopping probabilities. For example, Reach II (Jhongshan-Wudu) has the maximum overtopping probability of 0.811, whereas the overtopping probability of Reach IV (Yuanshanzi-Houtong) is the minimum (approximately 0.0) without the diversion. Nevertheless, with the Yuanshanzi diversion channel, Reach II still has the maximum overtopping probability (0.645), but its overtopping probability reduces from 0.811 to 0.645, and the corresponding reduction ratio approximates 30%.

Table 5 Regression coefficients in the maximum water-level relationship for four control points

Control point	α	*D_KD*	*D_JS*	*D_WD*	*D_YS*	NR_P	*TD*	*Cc*	$a^*_{T_{lag}}$	a^*_{weir}	*Nc*	n_f
Kwantu	1.431	0.047	−0.023	0.046	−0.039	0.018	0.923	−0.0002	−0.005	0.005	0.039	0.087
Jhongshan	1.141	0.0000	0.463	0.233	−0.256	0.214	0.275	0.011	0.006	−0.041	0.238	0.052
Wudu	2.256	0.000	0.000	0.769	−0.312	0.242	0.090	0.012	0.024	−0.074	0.174	0.010
Yuanshanzi	54.586	0.000	0.000	0.000	0.066	0.052	0.014	−0.0006	0.005	−0.013	0.030	0.002

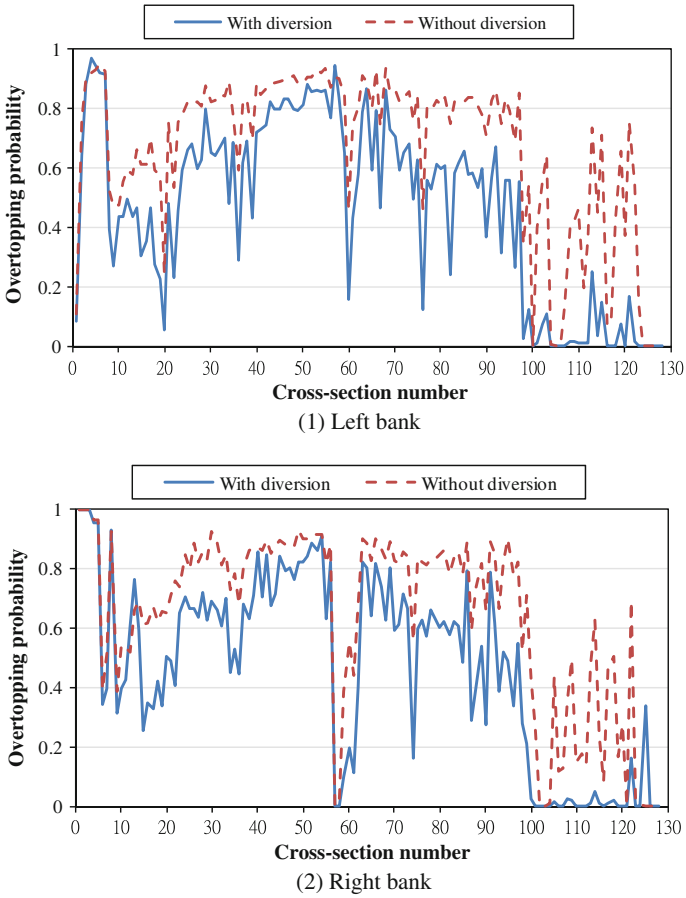

Fig. 8 Comparison of overtopping probability for levee system with and without Yuanshanzi flood-diversion channel

Although the diversion channel reduces the overtopping risk of the levees, the average overtopping probability approximates 0.5. According to the results of the uncertainty analysis for the 200-year rainfall amount through the bootstrap re-sampling method (see Fig. 9), the design values of the 200-year rainfall amounts at the four control points, 771 mm (Kwandu), 697 mm (Jhongshan), 773 mm (Wudu), and 815 mm (Yuanshanzi), approach the lower bound of the 95% confidence interval. In other words, the design values of the 200-year rainfall amounts at four control points are significantly underestimated, so that this probably results in a high overtopping probability. Hence, although the diversion channel effectively and significantly reduces the overtopping probability of the embankments, it is necessary to re-draft a flood protection and mitigation plan for severe flood events due to known or unpredicted uncertainties.

In conclusion, the proposed risk analysis model not only evaluates the reliability of the hydraulic structures due to uncertainties under the design flood, but also provides insightful information on the amendment of flood prevention and mitigations treatment plan on the Keelung River, especially for the reaches associated with high overtopping probabilities.

Table 6 Reach-wide average overtopping probabilities at four reaches and all cross-sections with and without flow-diversion channel

Reach	With diversion	Without diversion
(1) Left bank		
I Kwandu–Jhongshan (Sec. 1–18)	0.538	0.660
II Jhongshan–Wudu (Sec. 19–78)	0.645	0.811
III Wudu–Yuanshanzi (Sec. 79–124)	0.243	0.537
IV Yuanshanzi–Houtong (Sec. 125–128)	0.000	0.000
All cross-sections	0.465	0.666
(2) Right bank		
I Kwandu–Jhongshan (Sec. 1–18)	0.613	0.702
II Jhongshan–Wudu (Sec. 19–78)	0.624	0.787
III Wudu–Yuanshanzi (Sec. 79–124)	0.239	0.494
IV Yuanshanzi–Houtong (Sec. 125–128)	0.085	0.000
All cross-sections	0.467	0.645

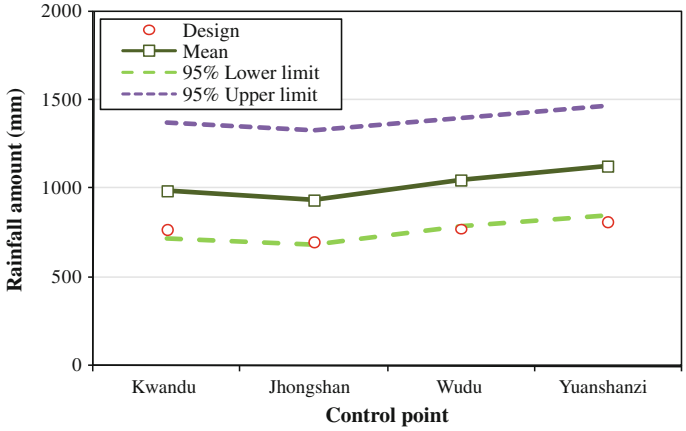

Fig. 9 Uncerainty analysis for 3-day, 200-year rainfall amount at four control points

3.4.2 Freeboard

A freeboard is commonly used in the design of an embankment or dam to reduce the overflow caused by wind-induced waves and the uncertainties unaccounted for. In general, the levees height equals the sum of the freeboard and the maximum water level corresponding to the design flood. In Taiwan, the 1.5 m freeboard is frequently adopted in the design of the embankment. However, the 1.5 m freeboard is just an empirical value without much basis or verification. Therefore, this study analyzes the effect of the freeboard on the overtopping probability as the freeboard increases from 0 to 1.5 m.

Figure 10 shows the overtopping probabilities on the two banks of the Keeling River under different freeboards. It can be seen that the overtopping probabilities on the both banks generally decrease with the increase in the freeboard for different cross-sections. On average, the overtopping probabilities decrease from 0.598 to 0.466 as the freeboard increases from 0 to 1.5 m. As shown in Table 7, the reach-wide average overtopping probability significantly drops with the increase in freeboards. For example, there are few

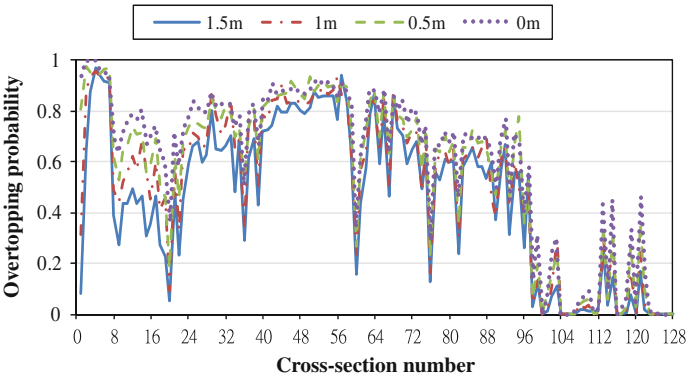

(1) Left bank

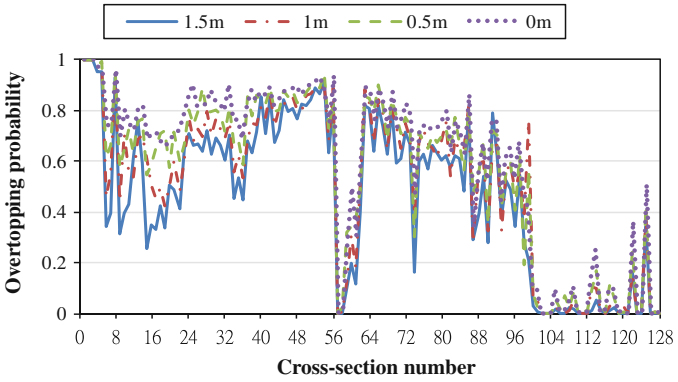

(2) Right bank

Fig. 10 Comparison of overtopping probabilities of levee system under various freeboards

Table 7 Reach-wide average overtopping probabilities in the four reaches and all cross-sections under various freeboards

Reach	Freeboard			
	0 m	0.5 m	1.0 m	1.5 m
(1) Left bank				
I Kwandu–Jhongshan (Sec. 1–18)	0.818	0.753	0.656	0.538
II Jhongshan–Wudu (Sec. 19–78)	0.782	0.744	0.703	0.645
III Wudu–Yuanshanzi (Sec. 79–124)	0.339	0.305	0.270	0.243
IV Yuanshanzi–Houtong (Sec. 125–128)	0.001	0.000	0.000	0.000
All cross-sections	0.603	0.565	0.519	0.465
(2) Right bank				
I Kwandu–Jhongshan (Sec. 1–18)	0.821	0.766	0.701	0.613
II Jhongshan–Wudu (Sec. 19–78)	0.763	0.724	0.673	0.624
III Wudu–Yuanshanzi (Sec. 79–124)	0.322	0.293	0.278	0.239
IV Yuanshanzi–Houtong (Sec. 125–128)	0.131	0.106	0.100	0.085
All cross-sections	0.592	0.556	0.517	0.467

visible improvements in the overtopping probabilities at Reach-IV (Yusnshanzi-Houtong). Nevertheless, the average overtopping probability at Reach-I (Kwandu-Jhongshan) decreases from 0.819 to 0.576 as the freeboards rise from 0 to 1.5 m. This is because the embankments at Reach-I is in the tidal-influenced zone in which downstream tide level dominates. Therefore, it is more useful to add the 1.5 m freeboard to prevent from the overtopping due to the tide.

This study indicates that through the proposed risk analysis model, the freeboard of 1.5 m is demonstrated to effectively reduce the overtopping probability of 22%, so that the freeboard is applicable to the design of the levee in Keelung River.

3.4.3 Scenario: 200-year rainfall amount due to climate change

Climate changes induced by global warming are expected to increase temperature, change precipitation patterns, and rise the frequency of extreme event (IPCC 2001). Climate change has been found to affect rainfall trends and increase the likelihood of flooding as well as the associated risk (Mansell 1997). Thus, the design values of the 200-year rainfall amount in the Keelung River obviously are underestimated so as to enhance the overtopping risk (see Fig. 9). Therefore, the effect of climate change on the 200-year rainfall amount must be explored, particularly as it relates to the performance of flood protection for the levees in the Keelung River. Booij (2005) pointed out that climate changes are systematic rather than random changes, and the large uncertainty range will be shifted to another level corresponding to the changed average situation. Hence, this study analyzes and quantifies the overtopping risk of the levees along the Keelung River for the scenario of increasing the mean values of the 200-year rainfall amounts attributed to climate change. Figure 11 shows the change in the overtopping probabilities along the left and right bank of the levee as 100 mm is added to the mean value of the 200-year rainfall amounts, 861 mm (Kwandu), 795 mm (Jhongshan), 868 mm (Wudu), and 928 mm (Yuanshanzi). On average, the overtopping probability rises from 0.465 to 0.765 with the increment of the average 200-year rainfall amount from 100 to 1,000 mm. The overtopping probability at Reach-II (Jhongshan-Kwandu) increases from 0.623 to 0.894 with the increase in the averaged 200-year rainfall amount, whereas Reach-IV (Yuanshanzi-Houtong) has an almost constant overtopping probability, approximating 0.005 (left bank) and 0.145 (right bank), respectively. As a result, an increase in the average 200-year rainfall amount due to climate change would significantly worsen the overtopping risk of the levees in the Keelung River.

In summary, the proposed risk model can quantify the effect of change in the average 200-year rainfall amount on the overtopping risk of the levees in the Keelung River. The Flood Protection and Mitigation Plan of the Keelung River might need amendment through upgrading the existing levee system based on the risk analysis results from the proposed model.

4 Conclusions

This study takes into account the uncertainty factors from hydrology, hydraulics, and geomorphology in determining the design flood to develop a risk analysis model for calculating the overtopping probability of the maximum water level rising over the levee crown by means of advanced first-order and second-moment (*AFOSM*) method. Specifically, The uncertainties considered involves the rainfall amount of a particular design

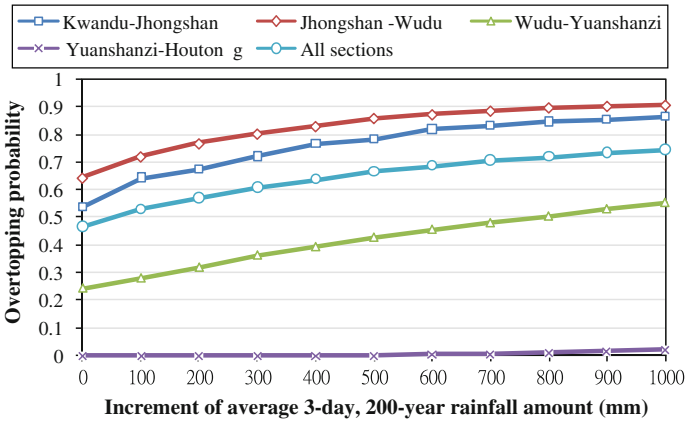

(1) Left bank

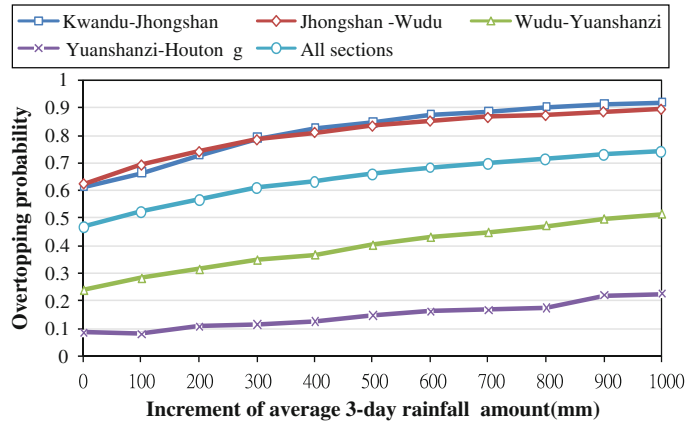

(2) Right bank

Fig. 11 Overtopping probability of levees under various increment of average 3-day, 200-year rainfall amount

return period, ordinates of design rainfall hyetograph (storm pattern), rainfall-runoff model parameters, downstream boundary (tide level), coefficients of the hydraulic structures (weir coefficient and contract coefficient of the bridge), Manning's roughness coefficient of the river bed, and infiltration (curve number).

The risk analysis model was implemented to assess the reliability of the flood-control capacity of the levee system, including the Yuanshanzi flood-diversion channel and freeboard, in Keelung River watershed considering hydrological, hydraulic, and geographical uncertainty factors. The results of the risk analysis from the proposed model, the 3-day, 200-year design rainfall amount and the maximum dimensionless rainfall of the design storm have more significant effect on the estimation of maximum water levels than the other uncertainty factors. The 1.5 m freeboard and the flood diversion could effectively enhance the reliability of flood-control capacity of the levees in the Keelung River. In addition, the proposed risk analysis successfully quantifies the overtopping risk of the levee system under a scenario, the increase in the average 200-year rainfall amount due to

climate change, and its results could be useful when planning to upgrade the existing levee system.

In this study, the uncertainty in river morphology is not considered. However, in reality, the river bed elevation and channel cross-sectional area can quickly and drastically change during flood events (Neuhold et al. 2009). As a result, changes in the river bed, as from the topographic data of the cross-section, could impact the estimation of the water level due to flooding. Therefore, the corresponding effect on the flood-control structures in the fluvial system could be evaluated through the proposed risk analysis model.

Acknowledgments The authors would like to express their appreciation to the Taiwan Water Resources Agency for providing the field data and for financial support under Project No. MOEAWRA0960199 'Evaluation of Risk Factors affecting the Functions of Hydraulic Structures (Except Storage structures) and Development of its Analysis Procedure'.

References

Anselmo V, Galeati G, Palmieri S, Rossi U, Todini E (1996) Flood risk assessment using and integrated hydrological and hydraulic modeling approach: a case study. J Hydrol 175:533–554

Apel H, Thieken AH, Merz B, Bloschl G (2004) Flood risk assessment and associated uncertainty. Nat Hazards Earth Syst Sci 4:295–308

Apel H, Thieken AH, Merz B, Bloschl G (2006) A probability modeling system for assessing flood risks. Nat Hazards 38(1–2):79–100

Apel H, Merz B, Thieken AH (2009) Influence of dike breaches on flood frequency estimation. Comput Geosci 35(5):907–923

Booij MJ (2005) Impact of climate change on river flooding assessed with different spatial model resolutions. J Hydrol 303:176–198

Cheng KS, Hueter I, Hsu EC, Yen HC (2001) A scale-invariant Gauss-Markov model for design storm hyetographs. J Am Water Resour As 37(3):723–736

Chou CM, Wang RY (2002) On-line estimation of unit hydrograph using the wavelet-based LMS algorithm. Hydrol Sci J 47(5):721–738

Gouldby B, Samuels P, Klijn F, Messner F, van Os A, Sayers P, Schanze J (2005) Language of risk. Project definitions. FLOODSite report, T32-04-01, p 56

Hadiani MO, Ebadi AG (2007) The role of land use changing in uncertainty of hydraulic structures. World Appl Sci J 2(2):136–141

IPCC (2001) Climate change 2001: the scientific basis. In: Houghton JT, Ding Y, Griggs DJ, Noguer M, van der Linden PJ, Dai X, Maskell K (eds) Contribution of working Group I to the third assessment report of the intergovernmental panel on climate change. Cambridge University Press, Cambridge

Keifer CJ, Chu HH (1957) Synthetic storm pattern for drainage design. ASCE J Hydraul Eng 83(4):1332/1–1332/24

Lee HL, Mays LW (1986) Hydraulic uncertainty in flood levee capacity. J Hydraul Eng 112(10):928–934

Mansell MG (1997) The effect of climate change on rainfall trends and flooding risk in the West of Scotland. Nordic Hydrol 28:37–50

Mays LW (2001) Stormwater collection system design handbook. McGraw-Hill, New York

National Research Council (2000) Risk analysis and uncertainty in flood damage reduction studies. National Academic Press, Washington, DC

Neuhold C, Stanzel P, Nachtnebel HP (2009) Incorporating river morphological change to flood risk assessment, uncertainty, methodology and application. Nat Hazards Earth Syst Sci 9:789–799

Rodriguez-Iturbe I, Gonzalez SM, Bras RL (1982) A geomorphoclimatic theory of instantaneous unit hydrograph. Water Resour Res 18(4):877–886

Salas JD, Burlando P, Heo JH, Lee DJ (2003) The axis of risk and uncertainty in hydrologic design. Hydrol Days 153–164

Schulz EF, Pinkayan S, Komsartra C (1971) Comparsion of dimensionless unit hydrographs in Thailand and Taiwan. Nordic Hydrol 2:23–46

Smith K, Ward R (1998) FLOODS: physical processes and human impacts. Wiley, New York

Snyder FF (1938) Synthetic unitgraphs. Trans Am Geophys Union 19:447–454

Soil Conservation Service (1972) National engineering handbook, section 4, Hydrology. US 444 Department of Agriculture, US Government Printing Office, Washington, DC
Tung YK (1985) Models for evaluating flow conveyance reliability of hydraulic structures. Water Resour Res 21:1463–1468
Tung YK, Mays LW (1981) Risk model for flood levee design. Water Resour Res 17(4):833–841
Uhlenbrook S, Seibert J, Leibundgut C, Rodhe A (1999) Prediction uncertainty of conceptual rainfall runoff models caused by problems in identifying model parameters and structure. Hydrol Sci J 44(5):779–797
Water Resources Agency (WRA) (2005) A review study of Keelung River basin regulation planning. Technologic report of Ministry of Economic Affairs, Taipei
WL|Delft Hydraulics (2005) SOBEK river/estuary user manual. SOBEK Help Desk
Wu CM (1965) Design untigraph for floods in Taiwan. Water Resources Planning Commission, Ministry of Economic Affairs, Taipei
Wu SJ, Tung YK, Yang JC (2006) Stochastic generation of hourly rainstorm events. Stoch Environ Res Risk Assess 21(2):195–212
Yen BC (1970) Risk in hydrologic design of engineering project. J Hydraul Div 96(4):959–966
Yen BC, Lee KT (1997) Unit hydrograph derivation for ungauged watershed by stream-order law. J Hydrol Eng 2(1):1–9
Yu ZB, White RA, Guo YJ, Voortman J, Kolb PJ, Miller DA, Miller A (2001) Stormflow simulation using a geographical information system with a distributed approach. J Am Water Resour As 37(44):957–971